J. Geophys. 43, 511–519, 1977

Journal of Geophysics

The Propagation of Plasma Waves in the Jovian Magnetosphere

K. U. Denskat and F. M. Neubauer

Institut für Geophysik und Meteorologie der Technischen Universität, Mendelssohnstr. 1 A, D-3300 Braunschweig, Federal Republic of Germany

Abstract. Plasma waves may conveniently be classified by constructing so called CMA diagrams. This approach was used to study broad band characteristics of plasma waves propagating in the Jovian magnetosphere. Spatial analogs of the well-known CMA diagrams show a large variety of different propagation conditions in the magnetospheric plasma in Jupiter's vicinity between 3 and 25 R_J. Among others the propagation regions of magneto hydrodynamic waves at low frequencies, "whistler" waves and regions with approximately vacuum propagation conditions can be delineated. In addition, the computations yield areas characterized by a total lack of wave activity.

As a possible source of wave generation and absorption cyclotron resonance interactions are of interest. The comparison of computed resonant particle energies necessary for cyclotron resonance with Pioneer observations of energetic particle fluxes illustrates the relevance of this mechanism as a source of wave generation and amplification in Jupiter's magnetosphere.

Key words: Jovian magnetosphere – Plasma wave propagation – CMA diagram.

Introduction

The Jupiter encounters by Pioneer 10 and 11 gave the first opportunity for in situ measurements of magnetic fields and particle populations in the Jovian magnetosphere. Our knowledge about Jupiter's magnetospheric conditions will be further improved and completed by future planetary missions like the Mariner-Jupiter-Saturn 77 mission to be launched this year and the Jupiter Orbiter Probe (JOP) to be launched in 1981/82.

An important diagnostic tool for probing the Jovian magnetosphere will be a plasma wave experiment. In the terrestrial magnetosphere the observation of the so-called ULF, ELF and VLF-emissions has yielded significant information on the processes determining the plasma physics of the magnetosphere. Waves observed by a suitable plasma wave experiment will have characteristics determined by the wave source and the propagation properties of the magnetosphere. It is the purpose of this paper to investigate the propagation characteristics of waves in the Jovian magnetosphere using the published Pioneer results on the magnetic field and the plasma distribution in the distance range from 3 to 25 Jovian radii (R_J). Since the above mentioned future missions do not penetrate to a distance closer than $\sim 6\ R_J$ (except for the atmospheric probe) we choose an upper limit of 100 kHz for the frequency range investigated. At several 100 kHz vacuum propagation conditions are essentially encountered outside $6\ R_J$. Propagation conditions above 100 kHz and below a radial distance of $6\ R_J$ have extensively been treated in theories of Jovian decametric emissions (e.g. Smith, 1975).

In the next section we describe the model for the magnetic field and plasma distribution which we have employed in our calculations.

Different wave propagation characteristics may be classified conveniently by constructing so-called CMA diagrams (e.g. Stix, 1962, Chap. 1 and 2). A spatial analog of this classification scheme may be used for waves propagating in the Jovian magnetosphere. Following this approach we computed configuration space CMA diagrams for specified frequencies. The results are shown in Section 3 and the implications for possible in situ observations are discussed.

Since cyclotron resonance interactions are expected to play an important role in the Jovian magnetosphere in the last section we present calculations on resonant energies for protons and electrons.

Magnetoplasma Models

According to the Pioneer vector magnetometer observations (Smith et al., 1974; Acuña and Ness, 1976) in the Jovian magnetosphere we can express the planetary magnetic field between 3 and 25 R_J by a dipole model with a moment $M = 4.0\ \text{Gauss} \cdot R_J^3$. We neglect the higher multipole moments which become progressively more important as the planet is approached. For simplicity we assume a centered dipole:

$$B = \frac{M}{r^3} \sqrt{1 + 3\cos^2 \vartheta}. \tag{1}$$

Here we have used the magnetic colatitude ϑ and radial distance r. This model may be oversimplified (e.g. No centrifugal drift currents which become noticeable outside about 15 R_J have been taken into account); however, the essential features of configuration space CMA diagrams are not expected to be affected by this simplification.

At present no reliable model of the density distribution of plasmas in the Jovian magnetosphere is available. We constructed an approximate interpolation formula for the magnetospheric plasma density from the Pioneer 10 low energy proton observations by Frank et al. (1976). However, this particle detector was designed to observe interplanetary plasmas. In addition, spacecraft charging may have been important (Scarf, 1975). Therefore, the observed plasma densities in Jupiter's magnetosphere are subject to some uncertainties and deviations from the density distributions reported are still possible.

The interpolation formula describes an electron-proton plasma with the density given by:

$$N = 0.1 + \frac{15}{P} + 50\left(\frac{3}{P}\right)^{2.3} + 8\,e^{-(P-6)^2} + 7\,e^{-\left(\frac{P-9.5}{1.3}\right)^2}\ \mathrm{cm}^{-3}. \tag{2}$$

P is defined as follows:

$$\begin{aligned} P &= \frac{r}{\mathrm{R_J}\sin^2\vartheta} && \text{for} \quad 3 \leqq P \leqq 10 \\ P &= -\frac{b}{a} + \sqrt{\frac{b^2}{a^2} - \frac{c}{a}} && \text{for} \quad 10 < P \leqq 25 \end{aligned} \tag{3}$$

with $a = \sin^2\vartheta + 3(\sin\vartheta)^{800}$

$b = 5\sin^2\vartheta - 15(\sin\vartheta)^{800} - 2r/\mathrm{R_J}$

$c = 20r/\mathrm{R_J}$

i.e. between the $\mathrm{L_J}$-shells (McIlwain's L-parameter) $\mathrm{L_J} = 3$ and $\mathrm{L_J} = 10$ we consider the density to be constant along a field line to $r = 3\ \mathrm{R_J}$. Outside $\mathrm{L_J} = 10$ the contours $N = \text{const}$ deviate from the field lines near the equator to form the "plasma sheet".

This formula takes into account the density enhancements around the $\mathrm{L_J}$-shells of Io and Europa and fits reasonably well the in situ observations by Frank et al. Figure 1 shows proton isodensity contours in the vicinity of Jupiter. The density gradient limiting the flux tube of Europa on the outside is somewhat steep. However, this gradient influences the configuration-space CMA diagrams only insignificantly.

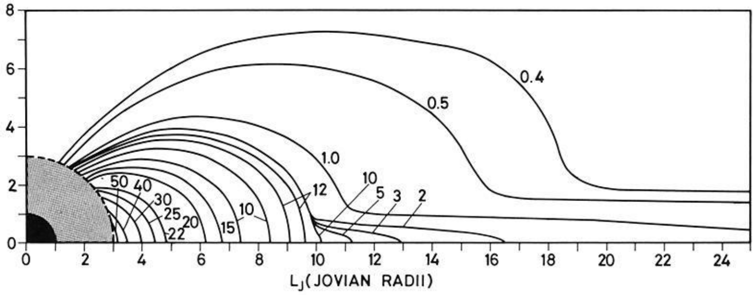

Fig. 1. Proton isodensity contours (in cm^{-3}) for the Jovian magnetosphere from 3 to 25 $\mathrm{R_J}$ computed from (2)

Wave Propagation and Configuration-Space CMA Diagrams in the Jovian Magnetosphere

The propagation properties of waves in a plasma depend on frequency, propagation direction and plasma properties. They are described by the refractive index $n = n(f, \Theta, N, B)$ in the case of a two-component cold plasma (f, Θ, N, B denote wave frequency, propagation angle relative to the magnetic field, electron and ion density of the plasma and magnetic field intensity, respectively). The dependence of n on these parameters is conveniently studied by investigating the form of $n(\Theta)$ at points in a appropriate space having scale lengths proportional to dimensionless quantities Ω_e^2/ω^2 and $(\Pi_i^2 + \Pi_e^2)/\omega^2$ where $\omega = 2\pi f$ and Ω_e, Π_i and Π_e are the angular electron cyclotron, ion plasma and electron plasma frequencies, respectively. Such a plot is called a CMA diagram (e.g. Stix, 1962). An example of a CMA diagram for an electron-ion plasma is shown in Figure 2. The parameter space is divided by lines called "bounding surfaces" which have special significance in determining the topological genera of the wave-normal surfaces $1/n(\Theta)$. Wave-normal surfaces are sketched inside each bounded volume, throughout which their topological genus remains unchanged.

The wave-normal surfaces for the two branches of n^2 are labeled right (R) or left (L) according to the sense of polarization at $\Theta = 0$, or ordinary (O) and extraordinary (X) according to the refractive index at $\Theta = \pi/2$. The topological genus to which a given branch of n^2 belongs depends on the coordinates in parameter space.

The bounding surfaces are constructed from the conditions for cutoff ($n^2 = 0$) and resonance ($n^2 = \infty$). These surfaces divide the parameter space into 13 volumes, each of which is characterized by its wave-normal surfaces. These volumes are sometimes referred to as plasma wave propagation ponds. For instance the propagation pond I contains vacuum propagation conditions in the lower left. The frequencies of waves in pond I are higher than any characteristic

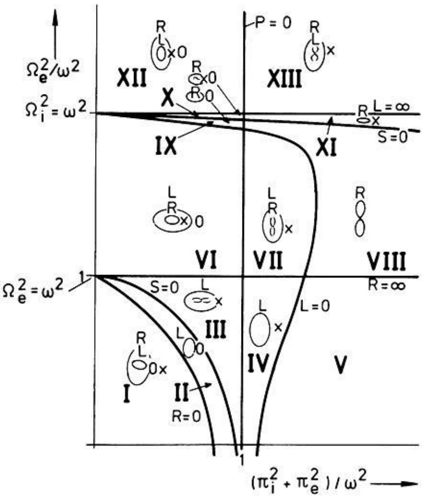

Fig. 2. CMA diagram for an electron-ion plasma (Stix, 1962). For convenience of presentation the ion-electron mass ratio was chosen to be 4. The bounding surfaces are given by the conditions for cutoff (R = 0, L = 0, and P = 0) and the principal resonances (R = ∞, L = ∞, and S = 0). Cross-sections of wave normal surfaces are sketched and labeled for each region. For these sketches the magnetic field is directed along the ordinate

frequency of the magnetoplasma. The opposite region XIII contains magnetohydrodynamic waves which have frequencies below any characteristic frequency. Waves well known as electron whistlers propagating between conjugate points in the earth's magnetosphere are found in region VIII.

To systematically classify wave propagation in planetary magnetospheres it proves convenient to construct spatial analogs to the parameter space CMA diagrams. Such configuration-space CMA diagrams for planetary magnetospheres allow an excellent overview over the spatial occurrence of different wave modes at specified frequencies. The boundaries in parameter space of Figure 2 now become spatial boundaries. Their significance also lies in the fact, that waves are reflected by cutoff surfaces and reflected or absorbed by resonance surfaces (Stix, 1962).

Using different plasma and magnetic field models Liemohn (1973) and Melander and Liemohn (1976) constructed configuration-space CMA diagrams for Jupiter's magnetosphere. In these papers theoretical plasma models of the Jovian magnetosphere were used which have not been confirmed by the Pioneer 10 observations by Frank et al. (1976) even under consideration of the measurement uncertainties mentioned above.

For specified frequencies ranging from 10 Hz to 10^5 Hz we computed the locations of bounding surfaces for cutoffs and the principal resonances in the Jovian magnetosphere using conventional cold plasma theory. Here we have neglected hot plasma effects which have to be taken into account if the perpendicular wavelength is not much greater than the particle gyroradii and if Landau and cyclotron resonance energies are not much greater than the average particle energy. This occurs e.g. near the resonance conditions $L = \pm\infty$ and $R = \pm\infty$ (notation after Stix, 1962) and will not further be discussed here. By Landau and cyclotron resonance energy we mean the kinetic energy of ions or electrons which are in Landau and cyclotron resonance, respectively, with the wave under consideration. For the simple cyclotron resonances some results are shown in the next section. In addition, in a hot plasma several new modes may appear like for example ion-acoustic waves, the significance of which depends on their instability and damping characteristics. Also we have neglected the possible role of heavy ions which may lead to extremely interesting propagation properties at very low frequencies.

Two configuration-space CMA diagrams are shown in Figures 3 and 4 for propagation frequencies of 100 Hz and 10 kHz. The labeling of bounding surfaces and the numbering of regions is retained from the parameter-space CMA diagrams. One can think of this diagram as having almost rotational symmetry with respect to the rotational axis of Jupiter in this part of the magnetosphere. In part this configuration-space CMA diagrams are completely different from the ones shown by Liemohn (1973) and Melander and Liemohn (1976) due to the different plasma distributions used. This concerns the locations of the bounding surfaces $R = 0$, $L = 0$ and $S = 0$. Of course, the locations of the bounding surfaces $R = \infty$ and $L = \infty$ are not affected by the choice of the plasma distribution.

At low frequencies (up to 1 kHz) there exist only a few large plasma wave propagation ponds each containing one wave genus in the Jovian magneto-

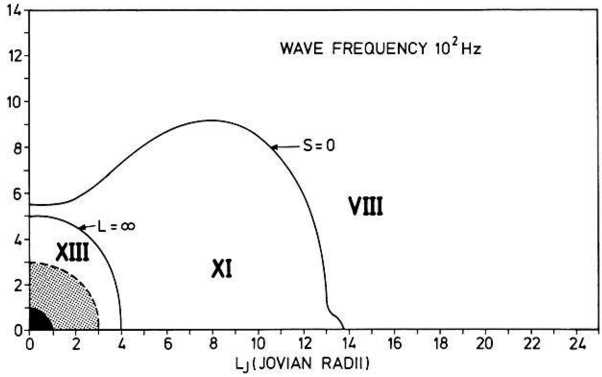

Fig. 3. Configuration-space CMA diagram in the Jovian magnetosphere for a wave propagation frequency of 100 Hz. The numbering of regions is the same as in Figure 2

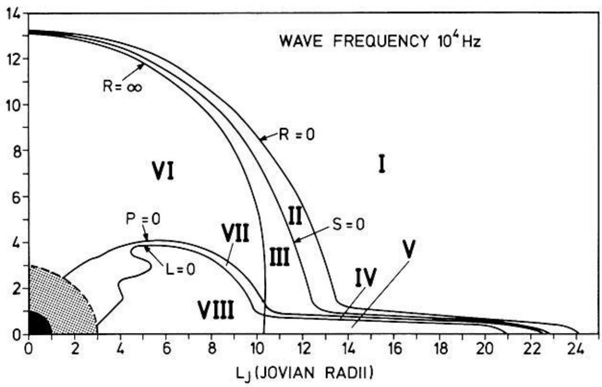

Fig. 4. Configuration-space CMA diagram in the Jovian magnetosphere for a wave propagation frequency of 10 kHz. The numbering of regions is the same as in Figure 2

sphere from 3 to 25 R_J. For a wave frequency $f=100$ Hz MHD wave propagation is possible in the innermost part of the magnetosphere (limited by the surface $L=\infty$). Region VIII denotes "whistler" wave propagation ponds.

A whistler wave propagating down the field line from the equatorial plane at $L_J=15$, say, will enter region XI by passing through the local lower hybrid resonance frequency ω_{LHR} ($S=0$) and enter the magnetohydrodynamic range XIII by passing through the proton gyro frequency ($L=\infty$). Also note, that propagation perpendicular to the magnetic field is not possible in region VIII.

We may consider waves propagating perpendicularly to the magnetic field in the equatorial plane from low altitudes. At $L_J \approx 14$ in the equatorial plane the lower hybrid frequency is reached where the wave is absorbed.

A large variety of plasma wave propagation ponds occurs at a frequency of 10 kHz. Particularly near the zenomagnetic equator regions of different topological wave genera are densely packed. For example, a spacecraft moving from intermediate magnetic latitude in the northern hemisphere through the zenomagnetic equator towards the southern hemisphere at $L_J=14$ will traverse five different propagation regions. Starting at almost vacuum propagation conditions, one wave mode (X or R) will disappear in region II, there are two modes again in region III. After passing through region IV with one wave mode the spacecraft will find itself in region V with no waves propagating at all followed by the reverse sequence. A region where no wave propagation is possible will be detected easily with broad band plasma wave receivers. At wave frequencies below 10 kHz even larger regions without any wave activity emerge remote from Jupiter (e.g. outside 22 R_J for a wave frequency of 1 kHz).

Because of the dipole tilt of ≈ 10 degrees the Galilean satellites will move between zenomagnetic latitudes ± 10 degrees. At 10 kHz Ganymede will periodically pass through regions I, II, III, IV, V. If it generates waves at 10 kHz they will be trapped in region V near Ganymede. It is only near the extreme latitude ± 10 degrees that 10 kHz waves can fill the outer magnetosphere.

Region II of the CMA diagram is the "stop-band" in models of Jovian decametric emissions. Its general significance lies in the fact that no extraordinary waves can propagate in this region. This is important because many mechanisms of wave generation produce exclusively extraordinary waves e.g. in region III. Since such waves have to reach region I and therefore have to pass through region II to be observed at the earth, region II acts as a "stop-band" (Smith, 1975) for extraordinary waves. Possibilities to overcome this problem have been discussed by Smith (1975) in terms of mode conversion, tunneling etc.

Cyclotron Resonance Interactions

Wave particle interactions are expected to be a major source of waves in the Jovian magnetosphere. Among the best known mechanisms are the cyclotron resonance interactions between electrons and ions and plasma waves.

Cyclotron resonance between a charged particle and a wave of frequency ω and wave vector $(k_\parallel, k_\perp)$ occurs when the particle with a velocity component $v_\parallel$ parallel to the steady background magnetic field B_0 fulfills the condition

$$\omega - k_\parallel v_\parallel + m\Omega_j = 0 \qquad m = 0, \pm 1, \pm 2, \ldots, \tag{4}$$

where $\Omega_j = |eB_0/m_j c|$ is the cyclotron frequency of the j-th species of charged particles.

To get an impression of the spatial energy distributions of particles needed for cyclotron resonance interactions in the Jovian magnetosphere we computed the necessary particle velocities parallel to the steady magnetic field from (4). We restricted the calculations to waves propagating parallel to the steady magnetic field for which only the simple cyclotron resonances $m = \pm 1$ in Equation (4) occur in the dispersion relations. To take relativistic particle velocities into account we replaced m_j by $m_{j0}/\sqrt{1 - v_\parallel^2/c^2}$ in (4) assuming particles with zero pitch-angle. The corresponding particle energies for 10 Hz and 10 kHz are shown in Figures 5 and 6 for electrons and protons in cyclotron resonance with the modes $n^2 = \mathrm{L}$ and $n^2 = \mathrm{R}$, respectively. Particle interactions with the L-mode are possible in region XIII of the CMA-diagram in Figure 5, interactions with the R-mode in regions VI to VIII of Figure 6 both under the assumption of zero pitch-angle.

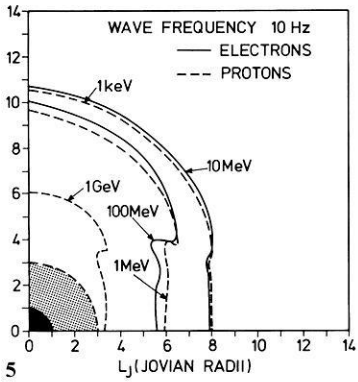

5

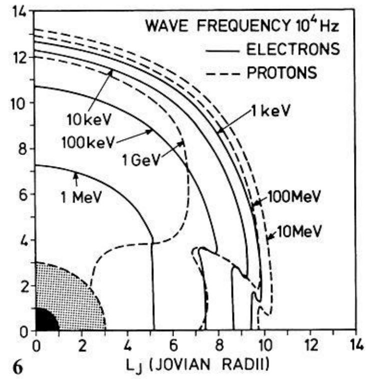

6

Fig. 5. Iso-energy contours in the Jovian magnetosphere for protons and electrons in cyclotron resonance with the L-mode for a wave propagation frequency of 10 Hz

Fig. 6. Iso-energy contours in the Jovian magnetosphere for protons and electrons in cyclotron resonance with the R-mode for a wave propagation frequency of 10 kHz

Pioneer 10 observations of energetic electrons and protons in the Jovian magnetosphere (Fillius and McIlwain, 1974; Trainor et al., 1974; Simpson et al., 1974) show significant particle fluxes in most of the magnetospheric regions and energy ranges considered in this study. These energetic particles may give rise to the generation and amplification of waves by cyclotron resonances (Scarf and Sanders, 1976; Barbosa and Coroniti, 1976).

Summary

Possible wave mode characteristics for Jovian magnetospheric waves have been evaluated at frequencies from 10 to 10^5 Hz. This frequency domain has been shown to contain a large variety of propagation conditions in Jupiter's magnetosphere from 3 to 25 R_J.

A classification of the different wave modes was done by using configuration-space CMA diagrams at specified frequencies (examples are shown for 10^2 Hz and 10^4 Hz).

The regions have been delineated in the Jovian magnetosphere, where plasma waves propagate as MHD-modes, "whistler" modes and where approximately "vacuum" propagation conditions with $n \approx 1$ for both possible modes characterize the propagation conditions. Also regions are defined in which no cold plasma propagation occurs.

Also we have studied the cyclotron resonance energies of protons and electrons at selected frequencies as a function of location. Particles at these resonance energies determine the absorption and instability characteristics of plasma waves in the Jovian magnetosphere for parallel propagation.

This study shows that the complex arrangement of the propagation regions in certain frequency ranges together with the resonant particle distributions will yield complex spatial patterns of magnetospheric waves. Vice versa these waves can be used by a wave experiment on a future mission to Jupiter to contribute to the understanding of the dynamical processes determining the particle population in the Jovian magnetosphere and the magnetoplasma distribution.

References

Acuña, M.H., Ness, N.F.: The main magnetic field of Jupiter. J. Geophys. Res. **81**, 2917–2922, 1976

Barbosa, D.D., Coroniti, F.V.: Relativistic electrons and whistlers in Jupiter's magnetosphere. J. Geophys. Res. **81**, 4531–4536, 1976

Fillius, R.W., McIlwain, C.E.: Measurements of the Jovian radiation belts. J. Geophys. Res. **79**, 3589–3599, 1974

Frank, L.A., Ackerson, K.L., Wolfe, J.H., Mihalov, J.D.: Observations of plasmas in the Jovian magnetosphere. J. Geophys. Res. **81**, 457–468, 1976

Liemohn, H.B.: Wave propagation in the magnetosphere of Jupiter. Astrophys. Space Sci. **20**, 417–429, 1973

Melander, B., Liemohn, H.: CMA propagation diagrams for the Jovian magnetosphere. Icarus **27**, 453–456, 1976

Scarf, F.L.: The magnetospheres of Jupiter and Saturn. In: The magnetospheres of the earth and Jupiter, Proc. Neil Brice Mem. Symp. (V. Formisano, ed.), pp. 433–449. Reidel 1975

Scarf, F.L., Sanders, N.L.: Some comments on the whistler mode instability at Jupiter. J. Geophys. Res. **81**, 1787–1790, 1976

Simpson, J.A., Hamilton, D.C., McKibben, R.B., Mogro-Campero, A., Pyle, K.R., Tuzzolino, A.J.: The protons and electrons trapped in the Jovian dipole magnetic field region and their interaction with Io. J. Geophys. Res. **79**, 3522–3544, 1974

Smith, E.J., Davis, L., Jr., Jones, D.E., Coleman, P.J., Jr., Colburn, D.S., Dyal, P., Sonett, C.P., Frandsen, A.M.A.: The planetary magnetic field and magnetosphere of Jupiter: Pioneer 10. J. Geophys. Res. **79**, 3501–3513, 1974

Smith, R.A.: Models of Jovian decametric radiation. In: Jupiter, studies of the interior, atmosphere, magnetosphere and satellites (T. Gehrels, ed.), pp. 1146–1189. Univ. Arizona Press 1976

Stix, T.H.: The theory of plasma waves. New York: McGraw-Hill 1962

Trainor, J.H., McDonald, F.B., Teegarden, B.J., Webber, W.R., Roelof, E.C.: Energetic particles in the Jovian magnetosphere. J. Geophys. Res. **79**, 3600–3613, 1974

Received December 27, 1976; Revised Version March 3, 1977